Talanta 86 (2011) 170–177

Contents lists available at SciVerse ScienceDirect

Talanta

journal homepage: www.elsevier.com/locate/talanta

Silica coated gold nanoaggregates prepared by reverse microemulsion method: Dual mode probes for multiplex immunoassay using SERS and fluorescence

Zhuyuan Wang, Shenfei Zong, Hui Chen, Hui Wu, Yiping Cui*

Advanced Photonics Center, Southeast University, Nanjing 210096, People's Republic of China

ARTICLE INFO

Article history:
Received 23 June 2011
Received in revised form 21 August 2011
Accepted 26 August 2011
Available online 1 September 2011

Keywords:
Surface enhanced Raman scattering
Fluorescence
Immunoassay
Reverse microemulsion method
Gold aggregates
Dual mode

ABSTRACT

A kind of fluorescent dye-doped, silica-coated Au aggregates was fabricated using reverse microemulsion method, which shows both strong fluorescence and intense surface enhanced Raman scattering (SERS) signals. Such a composite nanoparticle is composed of a SERS core as silica-coated Au aggregates and a fluorescent shell as dye-doped silica shell. Being prepared through reverse microemulsion method, the SERS core exhibits a sphere shape and a uniform size. Compared with a silica-coated single Au nanoparticle, our presented SERS core shows a greatly increased SERS intensity due to the Au aggregates, which is formed by simply mixing the SERS reporters and Au nanoparticles. When being excited at different wavelengths as 515 nm and 633 nm, the fluorescence and SERS signals can be separately generated, which can avoid the disturbance from each other. In addition, the potential application of such a dual mode nanoparticle in multiplex immunoassay was also demonstrated using a sandwiched structure, where the fluorescence mode can be used for indicating the occurrence of an immune reaction, and SERS mode can further be employed for distinguishing the specific kind of bio-analyte.

1. Introduction

The microarray immunoassay is a powerful tool for the analysis and characterization of biological samples, which has been widely used for clinical diagnostics, food safety, drug delivery, and environmental monitoring [1–3]. In recent years, multiplex immunoassay becomes more promising due to the rapid development of nanotechnology, in which multiple synthetic reactions and biological tests are performed simultaneously [4–6]. So far, several approaches have been employed for performing immunoassay detection, such as colorimetric [7], fluorescence [8], light scattering [9], surface plasmon resonance [10], electrochemical [11] and so on. Among these, the fluorescence-based immunoassay method has attracted most attention [12–14], which has the advantages of high-speed acquirement, easy performing and direct observation. Various fluorescent dyes can be used for multiplex labeling. However, because of the limited numbers of available fluorescent dyes with the same excitation wavelength and overlapping of the emission bands caused by broad emission profiles, some problems may be encountered when the number of analyte becomes large.

Recently, surface enhanced Raman scattering (SERS) has emerged as another sensitive method for bio-molecule analysis [15–18]. This technique has several advantages, including the richness of spectroscopic information with high resolution, the much narrower bandwidth and the non-photobleaching characteristics, which are especially advantageous for the detection in multiplex immunoassay [19]. Up to date, various types of metal nanoparticles have been explored in SERS-based immunoassays, such as nanospheres, nanorods, core–shell nanoparticles and so on [20–22]. Since the response of a SERS-based immunoassay is critically dependent on the SERS enhancing ability of the reporter-labeled metal nanoparticles, how to obtain a strong and stable SERS signal is of great importance. It has been reported that a remarkable surface enhancement effect can be generated by the aggregates in an appropriate size assembled by metal nanoparticles [23]. We have previously presented a SERS-based immunoassay by using the Raman reporter-labeled immuno-Au aggregates [24]. The results show that by simply mixing the Raman reporter of 4-mercaptobenzoic acid (4MBA) and Au nanoparticles, a stable Au aggregates can be obtained with an increased SERS intensity, which is advantageous in improving the sensitivity of a SERS-based immunoassay.

As mentioned above, both fluorescence and SERS spectroscopy have been successfully employed for detecting biomolecules. More recently, a new spectroscopy (or microscopy) technique, which uses the combined fluorescence and SERS signals, has emerged as an analytical tool with increased analytical capacity and sensitivity [25–28]. Considering the different advantages of fluorescence microscopy and SERS spectroscopy, this kind of dual mode spectroscopy holds great potential in the application of multiplex immunoassay.

* Corresponding author.
E-mail address: cyp@seu.edu.cn (Y. Cui).

0039-9140/$ – see front matter © 2011 Elsevier B.V. All rights reserved.
doi:10.1016/j.talanta.2011.08.054

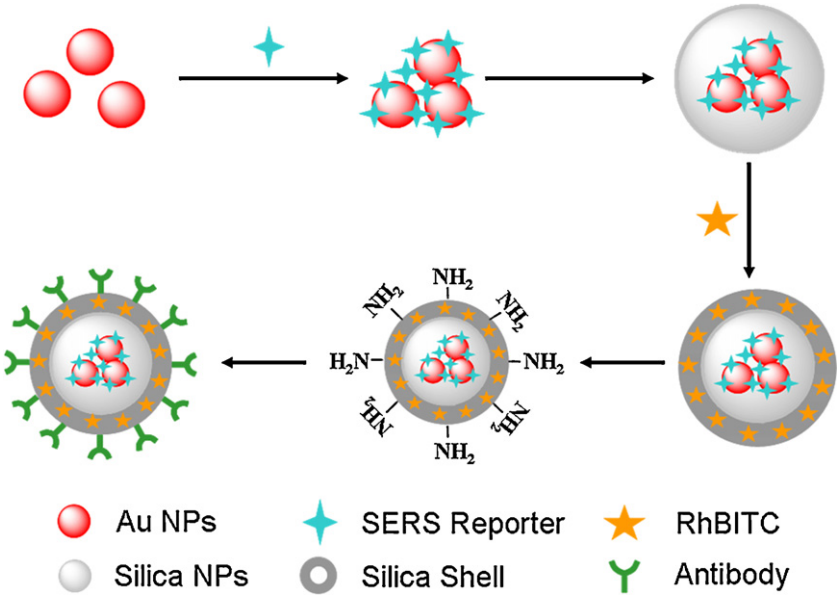

Scheme 1. Preparation of antibody-conjugated dual mode probes.

Here, we demonstrate a kind of dye-doped, silica-coated Au aggregates by using reverse microemulsion method, which show both strong fluorescence and intense SERS signals. Such a composite nanoparticle contains a SERS core as silica-coated Au aggregates and a fluorescent shell as dye-doped silica shell (shown in Scheme 1). Being prepared through reverse microemulsion method, the SERS core exhibits a sphere shape and a uniform size. Compared with a silica-coated single Au nanoparticle, our presented SERS core shows a greatly increased SERS intensity due to the Au aggregates, which is formed by simply mixing the SERS reporters and Au nanoparticles. When being excited at different wavelengths as 515 nm and 633 nm, the fluorescence and SERS signals can be separately generated, which can avoid the disturbance from each other. In addition, the potential application of such a dual mode nanoparticle in a multiplex immunoassay was also demonstrated using a sandwiched structure, where the fluorescence mode can be used for indicating the occurrence of an immune reaction, and SERS mode can further be employed for distinguishing the specific kind of bio-analyte.

2. Experimental

2.1. Materials

Triton X-100 and tetraethoxysilane (TEOS) were purchased from Alfa Aesar. Hydrogen tetrachloroaurate(III) trihydrate ($HAuCl_4{\cdot}3H_2O$), (3-aminopropyl) triethoxy-silane (APTES), rhodamine B isothiocyanate (RhBITC) and 5,5′-dithiobis(2-nitrobenzoic acid) (DTNB) were purchased from Sigma–Aldrich. Glutaraldehyde (GA, 25 wt.% aqueous solution) were purchased from Sinopharm Chemical Reagent CO., Ltd. Ammonium hydroxide was purchased from Shanghai Zhongshi Chemical Co., Ltd. Cyclohexane was purchased from Shanghai Shisihewei Chemical Co., Ltd. n-Hexanol was purchased from Shanghai Lingfeng Chemical Co. Ltd. 4-Mercaptobenzoic acid (4MBA) was purchased from Shanghai Dere Finechem Co., Ltd. Acetone was purchased from Shanghai Regent Co. Ltd. Sodium chloride was purchased from Shantou Xilong Chemical Co. Ltd. Bovine serum albumin (BSA), goat-anti-human IgG, goat-anti-mouse IgG, human IgG, mouse IgG and phosphate buffered saline (PBS, pH 7.4) were purchased from Nanjing Bookman Biotechnology Ltd. Deionized water (Millipore Milli-Q grade) with resistivity of 18.2 MΩ was used in all the experiments. All chemicals were used as received.

The borate buffered saline (BBS, pH 9.0) was prepared by dissolving disodium tetraborate decahydrate in de-ionized water with a final concentration of 2 mM. The PBST (containing 0.05% Tween 20) buffer solution was prepared by mixing Tween 20 with PBS buffer solution.

2.2. Preparation of silica-coated, SERS reporter-tagged gold aggregates (denoted as Au aggregates/DTNB@SiO_2 or Au aggregates/4MBA@SiO_2)

Colloidal gold was prepared according to the method developed by Frens [29]. The resulting gold nanoparticles showed an average diameter of ~15 nm according to the TEM images. 10 mL of the above gold colloidal was washed by centrifugation and re-suspended in 0.6 mL of water solution.

Then, the silica-coated, SERS reporter-tagged gold aggregates were prepared through a reverse microemulsion method with modifications [30]. First, microemulsion was prepared in a 250 mL three-neck flask consisting of 3.54 g of Triton X-100, 2.617 g of n-hexanol and 11.67 g of cyclohexane under vigorous stirring. Then, the as-prepared 0.6 mL of Au solution mixed with 400 μL of 10^{-2} M 4MBA (or DTNB) solution was injected into the microemulsion as soon as the color of the mixture turned from rose to blue. After the above mixed solution became clear, 100 μL of TEOS solution and 100 μL of ammonium hydroxide were added to initiate the polymerization reaction. The reaction was continued for 24 h under stirring. When the reaction was complete, the synthesized nanoparticles were isolated from the microemulsion using acetone, which were then centrifuged and washed with ethanol and water successively for several times to remove the surfactant and SERS reporters. Finally, the nanoparticles were re-suspended in 20 mL of ethanol.

2.3. Preparation of luminescent and SERS-activated silica nanospheres (denoted as Au aggregates/DTNB@SiO_2@RhBITC/SiO_2 or Au aggregates/4MBA@SiO_2@RhBITC/SiO_2)

Au aggregates/DTNB@SiO_2@RhBITC/SiO_2 and Au aggregates/4MBA@SiO_2@RhBITC/SiO_2 nanoparticles were fabricated through

a modified Stöber method [31]. In a typical experiment, 5 mL of the as-prepared Au aggregates/DTNB@SiO_2 or Au aggregates/4MBA@SiO_2 solution was added with 11 mL ethanol and 4 mL water, followed by the successive addition of RhBITC–APTES complex, 20 μL of TEOS and 190 of μL ammonium hydroxide. The mixture was kept stirring for 5 h. Here, the RhBITC–APTES complex was pre-prepared by adding 5 μL of APTES solution to 100 μL of RhBITC solution in ethanol, which was then reacted for 12 h in dark under continuous stirring. The resulting composite dual mode nanoparticles were washed by centrifugation and re-dispersed in ethanol.

2.4. Immunoassay protocols

2.4.1. Preparation of antibody conjugated dual mode nanoparticles

Goat-anti-human IgG and goat-anti-mouse IgG were conjugated with the dual mode nanoparticles through a same strategy. In the first step, Au aggregates/DTNB@SiO_2@RhBITC/SiO_2 and Au aggregates/4MBA@SiO_2@RhBITC/SiO_2 nanoparticles were both functionalized with amino groups by being mixed with APTES solution. Then, after being centrifuged for three times, these amino-modified nanoparticles were dispersed in water, followed by the addition of 4 mL GA. After the mixture was shaken for 2 h, the nanoparticles were washed thoroughly and dispersed in BBS. Then, 100 μL of the antibody (1 mg/mL in BBS) solution was added and the mixture was shaken at 25 °C for 2 h. Excess antibodies were removed by centrifugation. After being blocked with BSA (3% BSA in BBS), the purified nanoparticles was stored at 4 °C.

2.4.2. Preparation of immune substrates and immune reaction

In our experiments, the sandwich-type immunoassay chips were prepared as follows. First, the glass slides were sonicated in a piranha solution (75% H_2SO_4 and 25% H_2O_2) for 30 min and then rinsed with copious amount of deionized water. The cleaned glass slides were immersed in PEI solution (0.5% in PBS) for 2 h and rinsed with deionized water. Further, the slides were immersed in 2.5% GA aqueous solution for 3 h and rinsed with deionized water again. After the slides were dried with argon, 7 μL of goat-anti-human IgG and goat-anti-mouse IgG solutions (1 mg/mL in BBS) were pipetted onto two different spots on one slide, respectively, and incubated in a humidity chamber at 4 °C for 12 h. Afterwards, the glass slides were washed three times with PBST buffer and rinsed with deionized water to remove unbound antibodies. Nonspecific binding sites were blocked by immersing the slides in BSA solution (1% in BBS) for 3 h. Then, after the slides were washed with PBST solution and dried under argon, 7 μL of a mixed antigen solution, containing an equal volume of human IgG and mouse IgG (1 μg/mL in BBS), was pipetted onto the two antibody-immobilized spots and incubated at room temperature for 2 h. Again, the chips were washed with PBST solution and dried with argon. Then, 6.5 μL of the antibody-conjugated silica nanoparticles solution were pipetted onto the two antigens-modified spots and incubated at room temperature for 2 h. Finally, after being rinsed thoroughly to remove unbound nanoparticles and dried with argon, the chips were subjected to fluorescence and SERS measurements.

2.5. Instruments

Extinction spectra were measured by a Shimadzu UV-3600 PC spectrophotometer with quartz cuvettes of 1 cm path length. Photoluminescence emission spectra were measured by an Edinburg FLS 920 spectrofluorimeter. Transmission electron microscope (TEM) images were obtained with an FEI Tecnai G^2T20 electron microscope operating at 200 kV. Fluorescent images were recorded by confocal microscopy (FV 1000, Olympus) with a 10× microscope objective and the excitation wavelength is 515 nm. SERS spectra were recorded at 632.8 nm excitation (2.36 mW at the sample position) and Rayleigh scattering light was removed by a holographic notch filter. The Raman scattering light was directed to an Andor shamrock spectrograph equipped with a charge-coupled device (CCD).

3. Results and discussion

3.1. Characterization of silica-coated, SERS reporter-tagged Au aggregates (denoted as Au aggregates/DTNB@SiO_2 or Au aggregates/4MBA@SiO_2)

As reported previously, the aggregated metal nanoparticles show an increased SERS activity compared to the mono-dispersed one, due to the more formed "hot spots". In the structure of our proposed composite nanoparticles, Au aggregates were used as the core for an enhanced SERS performance. Although Au aggregates could be formed by adding the chloride ions to metal colloids, the process is usually uncontrollable and may result in particle precipitation. In our experiments, Au aggregates were fabricated by simply mixing the SERS reporter with Au nanoparticles. To demonstrate the wide applicability of such a protocol, DTNB and 4MBA were used as two examples. Using such a method, the Au aggregates containing a small number of nanoparticles can be achieved with strong SERS signals and good stability.

Fig. 1 shows two series of extinction spectra of Au nanoparticles in the time span of 40 min after they were added with DTNB and 4MBA molecules, respectively. It can be observed that with the increased time, the extinction peak of the Au nanoparticles (initially at ~530 nm) slightly bathochromically shifts after being tagged with DTNB or 4MBA. More importantly, there is a broad extinction band appeared at the red side of the spectra. As mentioned in Mie theory, the plasma resonance of the aggregates would result in an additional long wavelength component in the extinction spectrum, which distinguishes from the extinction of isolated nanoparticles dispersed in solution [32,33]. Besides, the Zeta-potential value of the citrate-capped Au nanoparticles was −54.5 mV and changed to −12.7 mV and −28.4 mV after being tagged with 4MBA and DTNB, respectively. Thus, it is deduced that both DTNB and 4MBA could induce the aggregation of Au nanoparticles. The reason may be explained as follows. Initially, the citrate-capped Au nanoparticles are stable in solution due to the electrostatic repulsion of their charged surface [34]. After being added with DTNB or 4MBA molecules, the citrate layers around Au nanoparticles are replaced by the DTNB or 4MBA layer through the formed Au–S bonds [35]. Then the negative surface charges formed by citrate ions are disrupted and the aggregation is induced via 'place exchange reaction' [36]. Comparing Fig. 1a with b, it can be found that the formation speed of Au aggregation induced by 4MBA is higher than that induced by DTNB, which may indicate a stronger interaction between 4MBA and Au nanoparticles. After 30 min, both DTNB- and 4MBA-induced aggregates stopped growing and began to keep stable in the solution, which can be deduced from their slightly changed extinction spectra after 30 min.

The resultant SERS reporters-induced Au aggregates were then incorporated within silica spheres using a modified reverse microemulsion method, forming uniform core/shell units with a spherical shape. In the experiments, to obtain the aggregates containing a small number of nanoparticles, the solution of SERS reporter-tagged Au nanoparticles were injected into the clear microemulsion right after they became blue in color. Fig. 2a shows the typical transmission electron microscopy (TEM) image of Au aggregates/DTNB@SiO_2 nanoparticles, which exhibit a spherical shape as well as a uniform size. The thickness of the silica shell

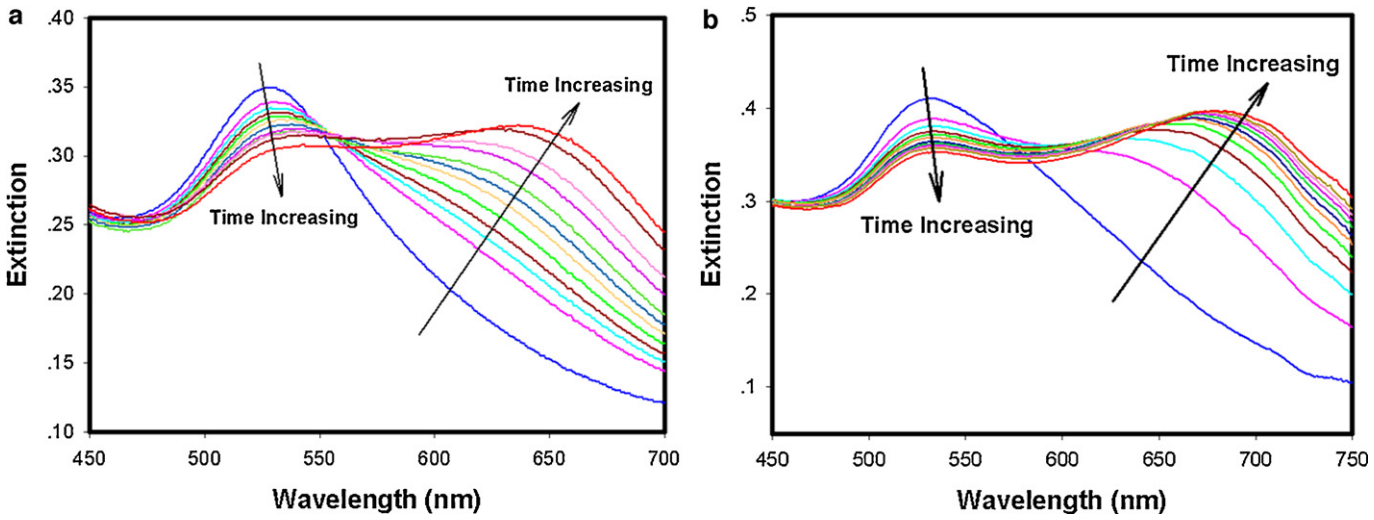

Fig. 1. Extinction spectra of Au nanoparticles (0.6 mL) upon the addition of DTNB (a) and 4MBA (b) solution (10^{-3} M, 2 mL) at different times as 1 min, 3 min, 6 min, 9 min, 12 min, 15 min, 18 min, 21 min, 24 min, 27 min, 30 min and 40 min.

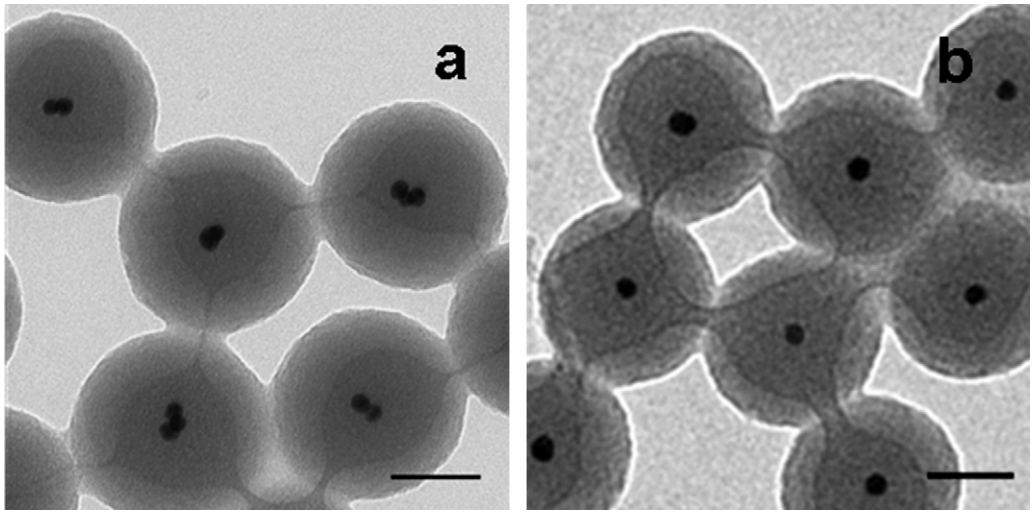

Fig. 2. TEM images of Au aggregates/DTNB@SiO_2 nanoparticles (a) and Au nanoparticle/DTNB@SiO_2 nanoparticles (b). The scale bar is 50 nm.

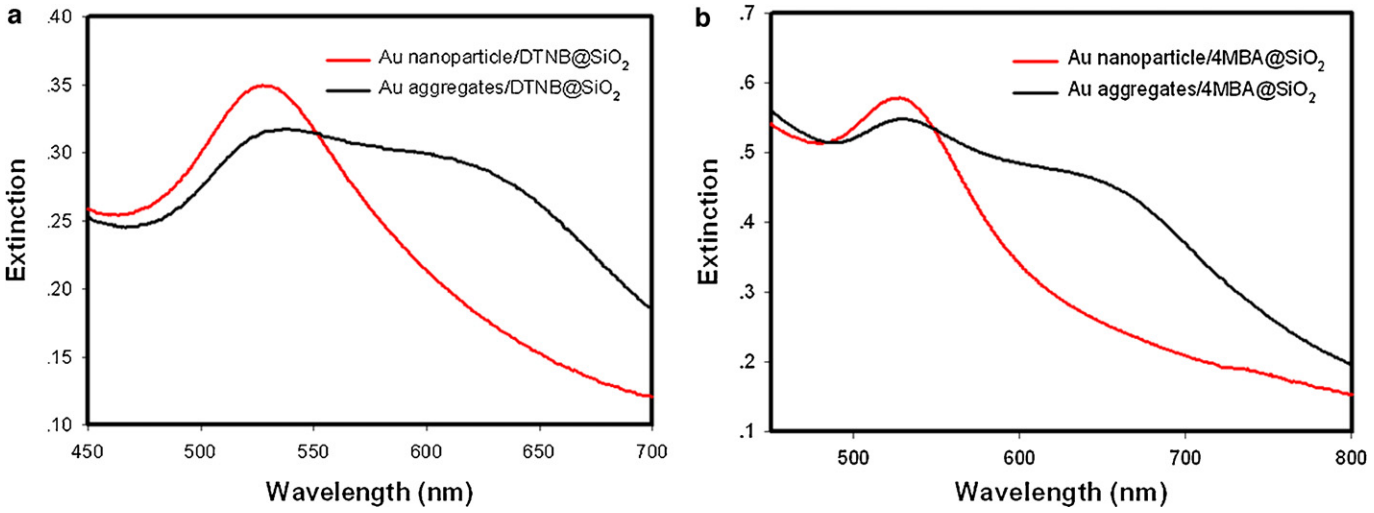

Fig. 3. Extinction spectra of Au aggregates/DTNB@SiO_2, Au nanoparticle/DTNB@SiO_2 (a) and Au aggregates/4MBA@SiO_2 nanoparticles, Au nanoparticle/4MBA@SiO_2 (b).

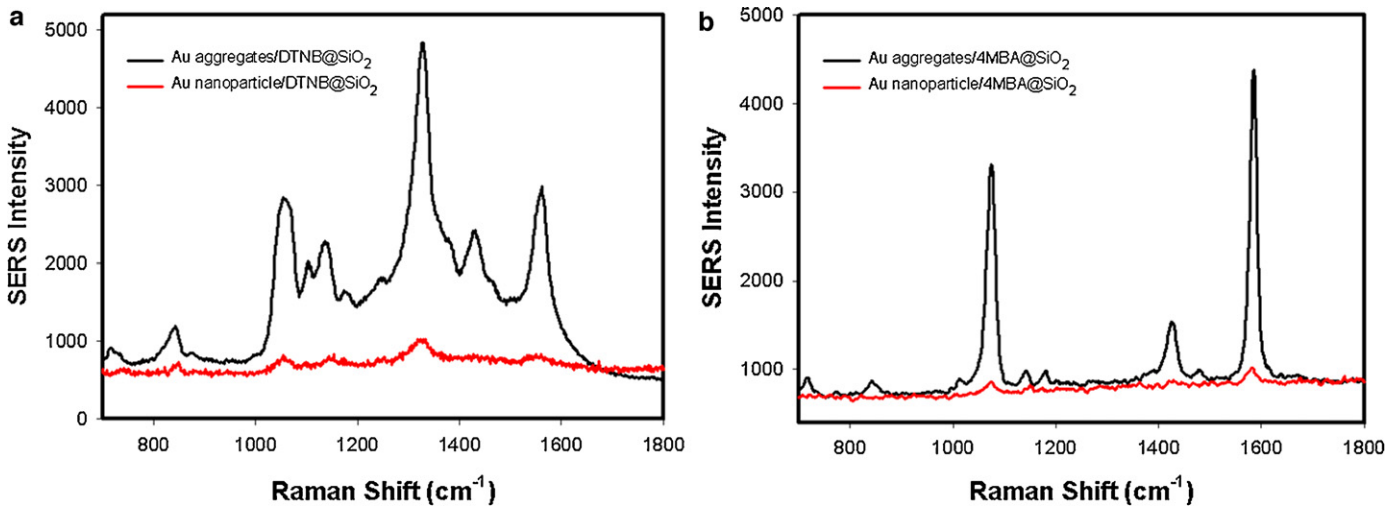

Fig. 4. SERS spectra of Au aggregates/DTNB@SiO_2, Au nanoparticle/DTNB@SiO_2 (a) and Au aggregates/4MBA@SiO_2 nanoparticles, Au nanoparticle/4MBA@SiO_2 (b).

can be tuned by changing the amount of tetraethyl orthosilicate (TEOS), the amount of ammonia solution, or the amount of aqueous solution of Au aggregates. The silica-coated Au aggregates used in this case had a silica-shell thickness of 50 nm on average, which had an average total diameter of about 120 nm. Moreover, the cores of such silica nanoparticles contain 2–3 aggregated Au nanoparticles. The aggregation state can also be indicated by the extinction spectra of silica nanoparticles, deduced from the shoulder located in the region above 600 nm (black curves in Fig. 3a and b).

The SERS performance of the prepared silica coated Au aggregates was investigated by using the excitation wavelength at 633 nm. The black curves in Fig. 4a and b show the SERS spectra of Au aggregates/DTNB@SiO_2 and Au aggregates/4MBA@SiO_2, respectively. Obviously, both the DTNB- and 4MBA-tagged Au aggregates remained their distinct SERS signals well after being incorporated within silica nanospheres. The SERS spectrum of DTNB is characterized by peaks at 1333 cm^{-1}, 1067 cm^{-1}, 1152 cm^{-1}, and 1558 cm^{-1}, which are assigned to the symmetric stretch of the nitro group, the succinimidyl N–C–O stretch overlapping with aromatic ring modes, the C–H deformation modes and the aromatic ring C–C stretching modes, respectively [37]. The SERS spectrum of 4MBA is dominated by peaks at 1077 cm^{-1}, 1590 cm^{-1} and 1434 cm^{-1}, which belong to the ring-breathing modes and the stretching mode of the carboxylate group [38]. It has been reported that as metal nanoparticles are brought together to form aggregates, their transition dipoles couple to each other. Thus, a significant SERS enhancement can often be observed at the junctions of two or more metal nanoparticles [39]. Usually, an enhanced signal detected at the junctions between nanoparticles of the aggregates is 2–40 times stronger than that obtained at an isolated nanoparticle [40,41].

Here, for a comparative study, we prepared two control samples as silica-coated Au nanoparticle, in which only one Au nanoparticle was encapsulated inside the silica shell (denoted as Au nanoparticle/DTNB@silica or Au nanoparticle/4MBA@silica). In the fabrication process, all the experimental parameters and conditions were kept the same as those for silica-coated Au aggregates, except that the 0.6 mL solution of Au colloids added with 400 μL solution of DTNB or 4MBA (10^{-2} M) was injected into the microemulsion immediately instead of waiting for its color to become blue. Both of the extinction spectra of Au nanoparticle/DTNB@silica and Au nanoparticle/4MBA@silica (the red curves in Fig. 3a and b) show that there was no obvious aggregation of Au nanoparticles being formed. The TEM image also proves that only a single Au nanoparticle was encapsulated in each silica nanosphere, as shown in Fig. 2b. SERS spectra of such nanoparticles are shown as the red curves in Fig. 4a and b, which were obtained by using the same integration time and laser power. Comparing the signal-to-noise ratios in Fig. 4a and b, it can be found that, by using Au aggregates as SERS cores instead of single Au nanoparticle, SERS activity has been enhanced by about 15 times.

3.2. *Characterization of luminescent and SERS-activated silica nanoparticles (denoted as Au aggregates/DTNB@SiO_2@RhBITC/SiO_2 or Au aggregates/4MBA@SiO_2@RhBITC/SiO_2)*

The resulting silica-coated Au aggregates were then coated with a layer of RhBITC-doped silica shell using a modified Stöber method. Fig. 5 shows the photoluminescence (PL) spectrum of Au aggregates/DTNB@SiO_2@RhBITC/SiO_2 nanoparticles, which was obtained by using an excitation wavelength at 515 nm. The emission peak is located at ~585 nm, indicating that the fluorescence of RhBITC remained well after being doped inside the outer silica shell.

Moreover, SERS spectra of Au aggregates/DTNB@SiO_2@RhBITC/SiO_2 and Au aggregates/4MBA@SiO_2@RhBITC/SiO_2 were both detected to investigate how the silica coating and fluorophore doping affect the SERS performance, as shown in Fig. 6a and b. The excitation wavelength was 633 nm. The result shows that due to the thick

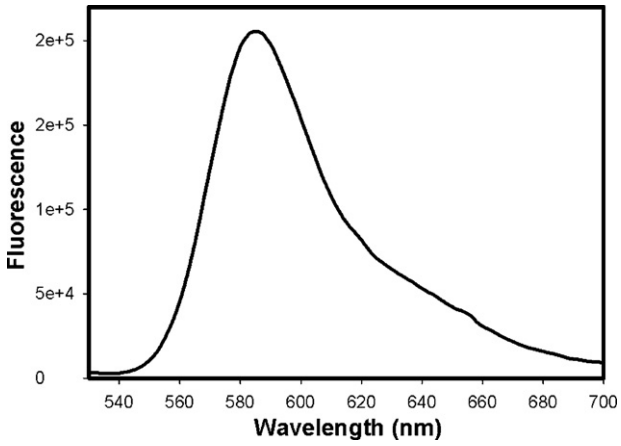

Fig. 5. PL spectrum of Au aggregates/DTNB@SiO_2@RhBITC/SiO_2.

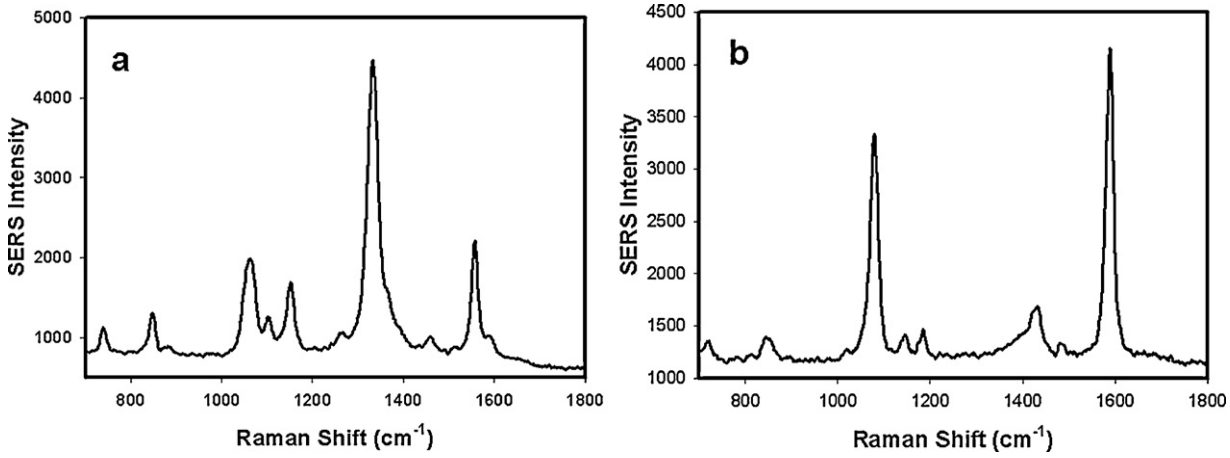

Fig. 6. SERS spectra of Au aggregates/DTNB@SiO_2@RhBITC/SiO_2 (a) and Au aggregates/4MBA@SiO_2@RhBITC/SiO_2 nanoparticles (b).

silica shell sandwiched between the DTNB- or 4MBA-tagged Au aggregates, strong SERS signals were retained well after the introduction of RhBITC-doped silica shell.

3.3. Application in multiplex immunoassay

To demonstrate the application of such dual mode nanoparticles in multiplex immunoassays, Au aggregates/DTNB@SiO_2@RhBITC/SiO_2 and Au aggregates/4MBA@SiO_2@RhBITC/SiO_2 were chosen as the models in a sandwiched immunoassay structure, which were conjugated with goat-anti-human IgG and goat-anti-mouse IgG, respectively. To avoid undesired adsorption, the empty sites on the surfaces of the nanospheres were blocked with bovine serum albumin (BSA). In the experiments, goat-anti-human IgG and goat-anti-mouse IgG were immobilized on two different regions in a chip, followed by the interaction with a mixed solution of human IgG and mouse IgG antigens. Afterwards, the goat-anti-human IgG-conjugated Au aggregates/DTNB@SiO_2@RhBITC/SiO_2 and goat-anti-mouse IgG-modified Au aggregates/4MBA@SiO_2@RhBITC/SiO_2 were pipetted onto two such chips for analysis. For checking the specificity, each chip was incubated with just one kind of the nanoparticles. After the reaction, the two chips were washed to remove the unbound analytes. Then, the fluorescence images and SERS spectra were obtained for each chip using excitation wavelengths of 515 nm and 633 nm, respectively. The results are shown in Fig. 7.

It can be seen that, on the chip pipetted with the goat-anti-human IgG-conjugated Au aggregates/DTNB@SiO_2@RhBITC/SiO_2, the goat-anti-human IgG-immobilized region show strong fluorescence and distinct SERS signals of DTNB, while goat-anti-mouse IgG-immobilized region show neglectable fluorescence or SERS signals (Fig. 7a), indicating the high specificities. Similarly, on the chip pipetted with the goat-anti-mouse IgG-conjugated Au aggregates/4MBA@SiO_2@RhBITC/SiO_2 nanoparticles, only the goat-anti-mouse IgG-immobilized region show strong fluorescence and distinct SERS signals of 4MBA (Fig. 7b). The above results indicate that such a kind of dual mode probe has potential applications in multiplex immunoassay. Specifically, when performing a detection of multiple bio-analyte, the fluorescence mode of such nanoparticles can be used for indicating the occurrence of an immune reaction, while the SERS mode can further be employed for distinguishing the specific kind of bio-analyte.

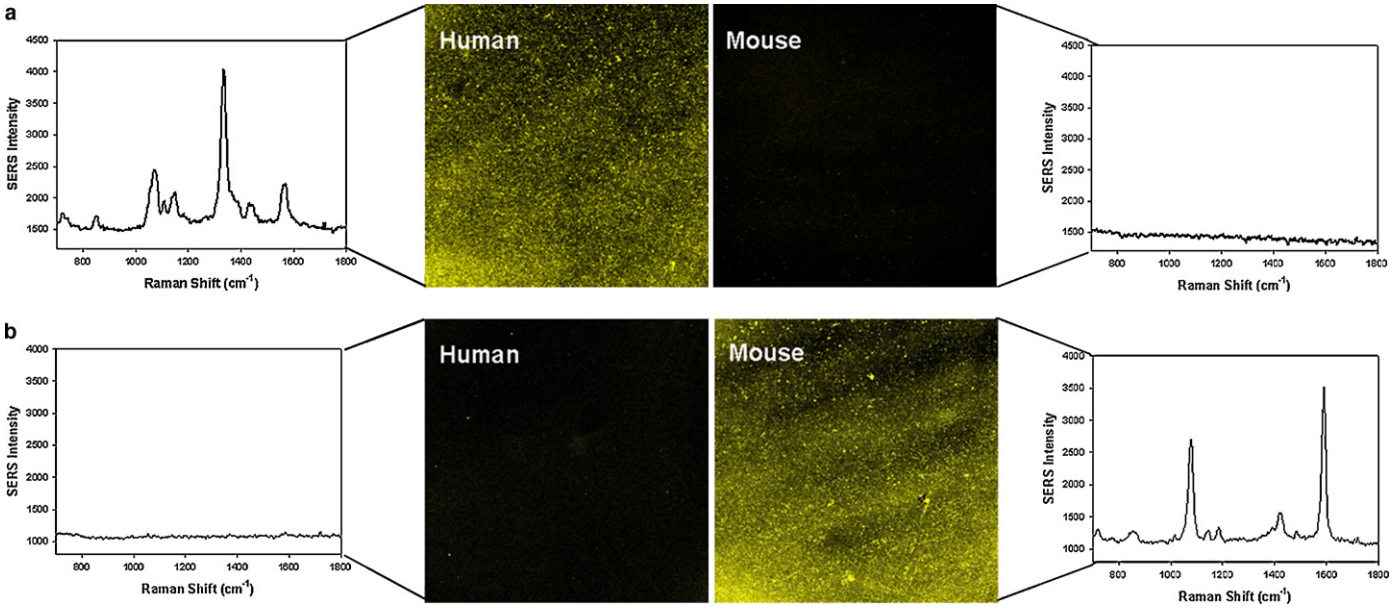

Fig. 7. Fluorescence images and SERS spectra of two sandwiched assays, which were pipetted with goat-anti-human IgG-modified Au aggregates/DTNB@SiO_2@RhBITC/SiO_2 nanoparticles (a) and goat-anti-mouse IgG-modified Au aggregates/4MBA@SiO_2@RhBITC/SiO_2 nanoparticles (b), respectively.

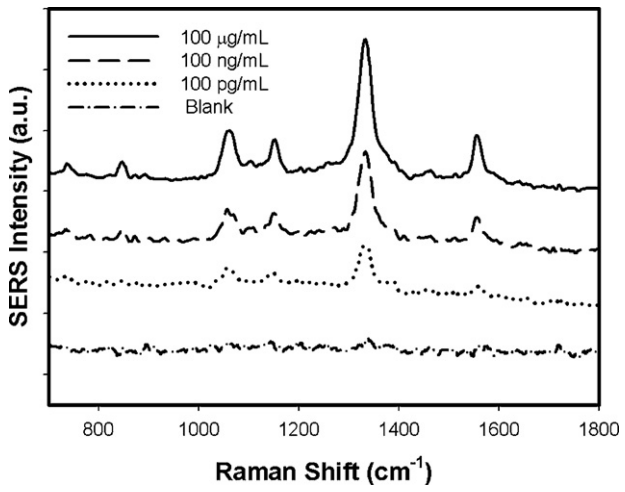

Fig. 8. Concentration-dependent SERS spectra for human IgG detection using the goat-anti-human IgG-conjugated Au aggregates/DTNB@SiO_2@RhBITC/SiO_2. The concentrations of human IgG are 100 μg/mL, 100 ng/mL and 100 pg/mL, respectively. The blank spectrum was obtained by replacing human IgG with BSA in the sandwich immunoassay.

Then, to explore the ability of such antibody-conjugated nanoparticles in quantitative bio-analysis, goat-anti-human IgG-conjugated Au aggregates/DTNB@SiO_2@RhBITC/SiO_2 was used as a model for the detection of human IgG in a sandwiched assay. In the experiments, human IgG with the concentration of 100 μg/mL, 100 ng/mL and 100 pg/mL were placed onto the goat-anti-human IgG incubated slides and then exposed to goat-anti-human IgG-conjugated Au aggregates/DTNB@SiO_2@RhBITC/SiO_2 nanoparticles. The concentration-dependent SERS spectra are shown in Fig. 8. The blank spectrum was obtained by replacing the human IgG antigen with BSA in the detection system. It can be observed that the intensity of SERS peaks from DTNB molecules increased concomitantly with the increasing concentration of the antigen. Distinct SERS signals from DTNB were detected even at a low human IgG concentration of 100 pg/mL. These results show that highly sensitive immunoassays are possible using such nanoparticles for quantitative detection of biomolecules.

4. Conclusion

In conclusion, we have demonstrated a kind of composite nanoparticles for multiplex immunoassay, operating through both strong fluorescence and SERS signals. In such a dual mode nanoparticles, silica-coated, SERS reporter-tagged Au aggregates serve as a core to generate SERS signals while an outer RhBITC-doped silica shell is used to provide fluorescence. Our experimental results show that both DTNB and 4MBA molecules have the ability to induce the aggregation of Au nanoparticles and to generate strong SERS signals. Then, being encapsulated with silica nanoparticles by reverse microemulsion method, the silica-coated Au aggregates have a spherical shape as well as a uniform size of ~120 nm. Compared with the silica nanoparticles containing a single Au nanoparticle, the silica-coated Au aggregates exhibit an increased SERS intensity of ~15 times. After being conjugated with specific antibodies, such dual mode nanoparticles were used to detect human IgG and mouse IgG antigens. Our experimental results show that the goat-anti-human IgG-conjugated Au aggregates/DTNB@SiO_2@RhBITC/SiO_2 can recognize specifically the human IgG antigens, which can be deduced by the SERS signals of DTNB and fluorescence of RhBITC. Similarly, the goat-anti-mouse IgG-conjugated Au aggregates/4MBA@SiO_2@RhBITC/SiO_2 nanoparticles only bound to the mouse IgG antigens, observed from the SERS signals of 4MBA and fluorescence of RhBITC. Therefore, these composite nanoparticles can be used as the indicator through both fluorescence and SERS, with high signal-to-noise ratio and high specificity.

We believe that the presented dual mode has potential application in multiplex biodetection, where fluorescence mode can be used for indicating the occurrence of an immune reaction, and SERS mode can further be employed for distinguishing the specific kind of bio-analyte.

Acknowledgements

This work was supported by Natural Science Foundation of China (NSFC) (Nos. 60708024, 60877024) and Specialized Research Fund for the Doctoral Program of Higher Education (SRFDP) (Nos. 20070286058, 20090092110015).

References

[1] P. Vicennati, N. Bensel, A. Wagner, C. Creminon, F. Taran, Angew. Chem. Int. Ed. 44 (2005) 6863–6866.
[2] L.A. Rivas, J. Aguirre, Y. Blanco, E. Gonzalez-Toril, V. Parro, Environ. Microbiol. 13 (2011) 1421–1432.
[3] L.J. Kricka, Clin. Chem. 38 (1992) 327–328.
[4] D.C. Pregibon, M. Toner, P.S. Doyle, Science 315 (2007) 1393–1396.
[5] X.D. Lou, G.H. Zhang, I. Herrera, R. Kinach, O. Ornatsky, V. Baranov, M. Nitz, M.A. Winnik, Angew. Chem. Int. Ed. 46 (2007) 6111–6114.
[6] V. Mani, B.V. Chikkaveeraiah, V. Patel, J.S. Gutkind, J.F. Rusling, ACS Nano 3 (2009) 585–594.
[7] J. Wang, Y. Cao, Y.Y. Xu, G.X. Li, Biosens. Bioelectron. 25 (2009) 532–536.
[8] M.C. Pirrung, R.V. Connors, A.L. Odenbaugh, M.P. Montague-Smith, N.G. Walcott, J.J. Tollett, J. Am. Chem. Soc. 122 (2000) 1873–1882.
[9] X. Liu, Q. Dai, L. Austin, J. Coutts, G. Knowles, J.H. Zou, H. Chen, Q. Huo, J. Am. Chem. Soc. 130 (2008) 2780–2782.
[10] K.S. Phillips, T. Wilkop, J.J. Wu, R.O. Al-Kaysi, Q. Cheng, J. Am. Chem. Soc. 128 (2006) 9590–9591.
[11] D.P. Tang, B.L. Su, J. Tang, J.J. Ren, G.N. Chen, Anal. Chem. 82 (2010) 1527–1534.
[12] J. Yan, M.C. Estévez, J.E. Smith, K. Wang, X. He, L. Wang, W. Tan, Nanotoday 2 (2007) 44–50.
[13] J. Li, Z.Y. Wang, I. Gryczynski, W. Mandecki, Anal. Bioanal. Chem. 398 (2010) 1993–2001.
[14] C.S. Huang, S. George, M. Lu, V. Chaudhery, R.M. Tan, R.C. Zangar, B.T. Cunningham, Anal. Chem. 83 (2011) 1425–1430.
[15] C.I. Brady, N.H. Mack, L.O. Brown, S.K. Doorn, Anal. Chem. 81 (2009) 7181–7188.
[16] B.R. Lutz, C.E. Dentinger, L.N. Nguyen, L. Sun, J.W. Zhang, A.N. Allen, S. Chan, B.S. Knudsen, ACS Nano 2 (2008) 2306–2314.
[17] M. Manimaran, N.R. Jana, J. Raman Spectrosc. 38 (2007) 1326–1331.
[18] Z.Y. Wang, S.F. Zong, J. Yang, J. Li, Y.P. Cui, Biosens. Bioelectron. 26 (2011) 2883–2889.
[19] S.M. Nie, S.R. Emery, Science 275 (1997) 1102–1106.
[20] J. Neng, M.H. Harpster, H. Zhang, J.O. Mecham, W.C. Wilson, P.A. Johnson, Biosens. Bioelectron. 26 (2010) 1009–1015.
[21] N.N. Yazgan, I.H. Boyaci, E. Temur, U. Tamer, A. Topcu, Talanta 82 (2010) 631–639.
[22] B.H. Jun, J.H. Kim, H. Park, J.S. Kim, K.N. Yu, S.M. Lee, H. Choi, S.Y. Kwak, Y.K. Kim, D.H. Jeong, M.H. Cho, Y.S. Lee, J. Comb. Chem. 9 (2007) 237–244.
[23] X.B. Tan, Z.Y. Wang, J. Yang, C.Y. Song, R.H. Zhang, Y.P. Cui, Nanotechnology 20 (2009) 445102.
[24] C.Y. Song, Z.Y. Wang, R.H. Zhang, J. Yang, X.B. Tan, Y.P. Cui, Biosens. Bioelectron. 25 (2009) 826–831.
[25] M.A. Woo, S.M. Lee, G. Kim, J. Baek, M.S. Noh, J.E. Kim, S.J. Park, A. Minai-Tehrani, S.C. Park, Y.T. Seo, Y.K. Kim, Y.S. Lee, D.H. Jeong, M.H. Cho, Anal. Chem. 81 (2009) 1008–1015.
[26] Z.Y. Wang, H. Wu, C.L. Wang, S.H. Xu, Y.P. Cui, J. Mater. Chem. 21 (2011) 4307–4313.
[27] A. Pallaoro, G.B. Braun, N.O. Reich, M. Moskovits, Small 6 (2010) 618–622.
[28] K. Kim, H.B. Lee, J.Y. Choi, K.S. Shin, ACS Appl. Mater. Interfaces 3 (2011) 324–330.
[29] G. Frens, Nat. Phys. Sci. 241 (1973) 20–22.
[30] R.P. Bagwe, C. Yang, L.R. Hilliard, W. Tan, Langmuir 20 (2004) 8336–8342.
[31] A.V. Blaaderen, A. Vrij, Langmuir 8 (1992) 2921–2931.
[32] G. Mie, Ann. Phys. 25 (1908) 377–445.
[33] P. Galletto, P.F. Brevet, H.H. Girault, R. Antoine, M. Broyer, J. Phys. Chem. B 103 (1999) 8706–8710.
[34] S. Basu, S. Pande, S. Jana, S. Bolisetty, T. Pal, Langmuir 24 (2008) 5562–5568.

[35] S. Jang, J. Park, S. Shin, C. Yoon, B.K. Choi, M.S. Gong, S.W. Joo, Langmuir 20 (2004) 1922–1927.
[36] S. Basu, S.K. Ghosh, S. Kundu, S. Panigrahi, S. Praharaj, S. Pande, S. Jana, T. Pal, J. Colloid Interface Sci. 313 (2007) 724–734.
[37] D.S. Grubisha, R.J. Lipert, H.Y. Park, J. Driskell, M.D. Porter, Anal. Chem. 75 (2003) 5936–5943.
[38] A. Michota, J. Bukowska, J. Raman Spectrosc. 34 (2003) 21–25.
[39] A.M. Michaels, J. Jiang, L. Brus, J. Phys. Chem. B 104 (2000) 11965–11971.
[40] Q. Zhou, G. Zhao, Y. Chao, Y.L. Wu, J. Zheng, J. Phys. Chem. C 111 (2007) 1951–1954.
[41] F. Svedberg, Z. Li, H. Xu, M. Kall, Nano Lett. 6 (2006) 2639–2641.